Structure 14, 1527–1534, October 2006 ©2006 Elsevier Ltd All rights reserved DOI 10.1016/j.str.2006.08.004

Kinking Occurs during Molecular Dynamics Simulations of Small DNA Minicircles

Filip Lankaš,[1] Richard Lavery,[2] and John H. Maddocks[1,*]
[1] Laboratory for Computation and Visualization in Mathematics and Mechanics
Institut de Mathématiques B
Ecole Polytechnique Fédérale de Lausanne
CH-1015 Lausanne
Switzerland
[2] Laboratoire de Biochimie Théorique
CNRS UPR 9080
Institut de Biologie Physico-Chimique
Paris 75005
France

Summary

Recent experiments on minicircle formation suggest that a conformational mechanism other than smooth deformation may be playing a role in enhancing DNA flexibility. Both local base unpairing and kink formation have been suggested as possible explanations. Although kinks within isolated DNA were proposed 30 years ago, they have, until now, only been observed within DNA complexed with proteins. In order to test how DNA behaves in the strong bending regime, we have carried out molecular dynamics simulations of a 94 base pair minicircle in explicit solvent with two different linking numbers, corresponding to a torsionally relaxed state and a positively supercoiled state. The simulations suggest that sharp kinks can indeed arise in small minicircles. The relaxed minicircle is generally associated with a single kink, while two kinks occur with the supercoiled state. No evidence is seen of base unpaired regions.

Introduction

The mechanical properties of double-stranded DNA are of considerable interest given the deformations that are imposed on this vital biological polymer in its natural cellular environment. DNA already departs from its ideal, regular helical structure on a local scale due to base sequence effects. It is also susceptible to deformation resulting from thermal agitation, interactions with small ligands, or with DNA binding proteins. On a larger scale, protein binding can also induce DNA looping (Vilar and Saiz, 2005) and DNA packaging (Richmond and Davey, 2003), both of which play important roles in gene expression.

It has been demonstrated that at length scales of many multiples of its persistence length (i.e., at scales far beyond 50 nm or 150 base pairs, or bp), DNA can be well described with the classic models of polymer physics (Doi and Edwards, 1985; Shimada and Yamakawa, 1984), provided that it is not subjected to significant longitudinal (Cluzel et al., 1996; Smith et al., 1996) or torsional stress (Allemand et al., 1998; Strick et al., 1996). The so-called worm-like chain (WLC) model (Kratky and Porod, 1949), which treats DNA as a semi-flexible polymer with a defined bending modulus, has been shown to perform particularly well in this respect (Bustamante et al., 1994; Vologodskii, 1994).

At shorter scales, heteropolymer models involving elastic rod theories with quadratic energies that include sequence-dependent intrinsic shape and stiffness parameters can capture experimental measurements of cyclization probabilities, or J factors, of DNA minicircles of lengths in the range 150–200 bp; that is at, or slightly above, a single persistence length (Manning et al., 1996; Zhang and Crothers, 2003). These models implicitly assume a relatively smooth deformation of the DNA double helix with comparatively small deformations from the intrinsic helical geometry of each base-pair step. However, the maximum curvature for which such continuum descriptions are a good approximation is unclear. A possible answer to this question comes from recent experiments investigating the cyclization probabilities of DNA fragments of roughly 100 bp in length (Cloutier and Widom, 2004, 2005). These experiments suggest that such fragments can form minicircles orders of magnitude more easily than WLC or continuum models predict. This finding has already prompted the development of extended WLC models that allow for increased flexibility either by including locally unpaired segments of the helix (Yan et al., 2005; Yan and Marko, 2004) or by allowing for the formation of kinks (Wiggins et al., 2005), as was originally predicted by Crick and Klug some 30 years ago (Crick and Klug, 1975). A recent publication (Du et al., 2005) has questioned the kinetic analysis of the cyclization experiments (Cloutier and Widom, 2004, 2005) and makes further verifications necessary. Du et al. also suggested that sharp kinks would only occur with very low probabilities; but it should be noted that their conclusion depends on the detailed conformational and mechanical properties of the kinks, which remain unclear at present.

It is known from structural studies that various degrees of DNA kinking occur within a wide variety of protein-DNA complexes, notably within the 147 bp of DNA tightly wrapped in roughly 1.7 turns around the nucleosome core particle (Richmond and Davey, 2003). Such kinks involve the formation of negative roll angles between consecutive base pairs, opening the major groove side of the base-pair step and cause kinking toward the minor groove. It is also found that kinks tend to appear where the base stacking is weakest, generally at pyrimidine-purine steps (commonly abbreviated as YpR) and, more specifically, at the thermodynamically weakest TpA step (Drew et al., 1985; Protozanova et al., 2004; Travers, 2005). In addition, experiments on DNA looping, with loops that frequently contain less than 100 bp, show that protein binding appears to be necessary to modulate the torsional flexibility of DNA, but not to modulate its bending (Becker et al., 2005). This observation can again be interpreted as evidence in favor of spontaneous kink formation.

*Correspondence: john.maddocks@epfl.ch

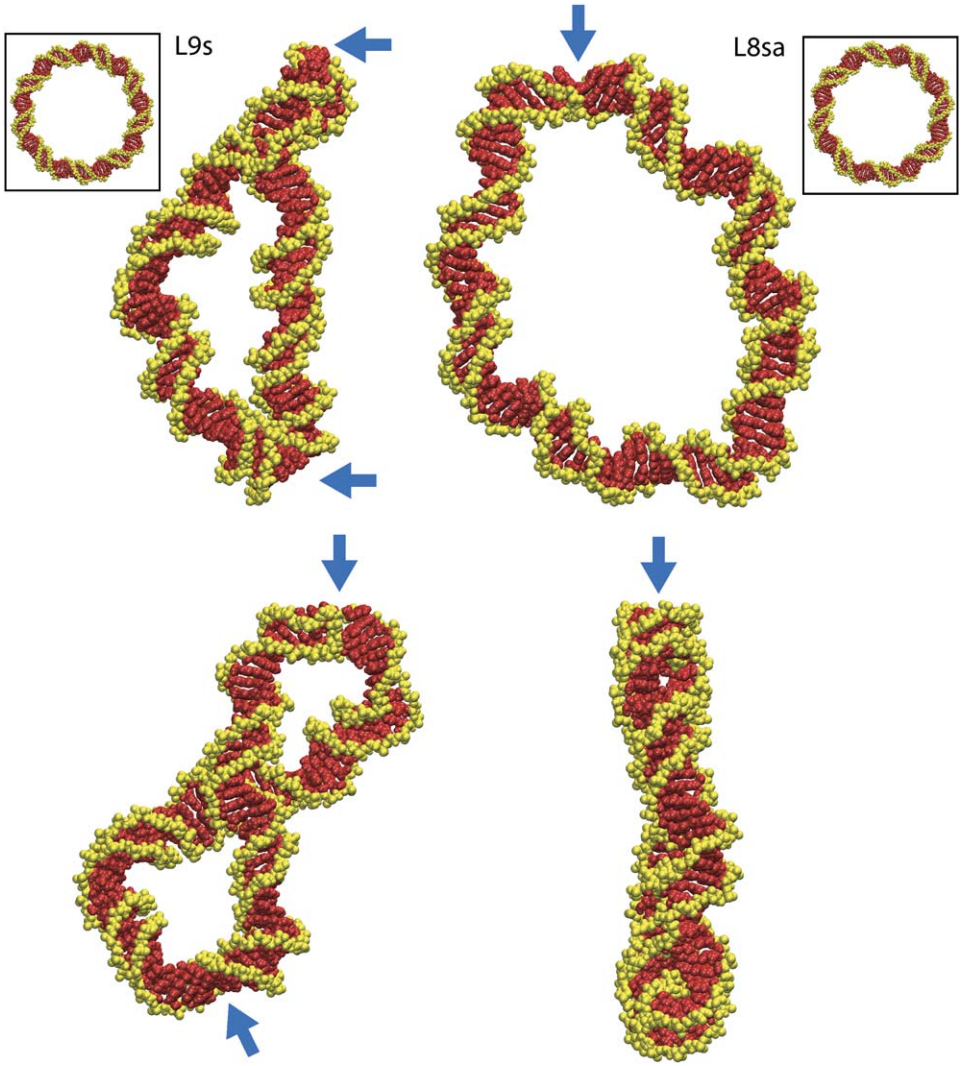

Figure 1. Minicircle Conformations after 80 ns of Simulation

On the left, two views of the swiss-roll configuration of L9s with the two projections differing by a rotation of 90° about the vertical, and on the right, the analogous views of the teardrop of L8sa. (PDB files and movies of these three-dimensional structures are provided in the Supplemental Data.) Kink positions are indicated by arrows. For both simulations, the almost circular starting structure is shown in the inserts.

In order to try and further clarify the situation for isolated, strongly bent DNA, we have chosen to carry out atomic-resolution molecular dynamics simulations of one of the 94 bp sequences studied in the cyclization experiments of the Widom group (Cloutier and Widom, 2004, 2005). Our simulations use a refined force field, which has been extensively tested for nucleic acids, and an explicit representation of the solvent and counterion environment surrounding the DNA molecule. Although a DNA minicircle is a large molecule in simulation terms, we have carried out several independent trajectories of 80 ns or more, longer than the vast majority of molecular dynamics studies performed on DNA until now. We have performed simulations on minicircles with two different degrees of supercoiling (i.e., with two different linking numbers, *Lk*) in order to judge the effect of this change on the minicircle conformations.

Our results suggest that local kinking involving one or two adjacent base-pair steps will spontaneously form in DNA minicircles of approximately 100 bp. The kinks, like those observed in protein-DNA complexes, bend DNA toward the minor groove and appear to form preferentially at YpR steps. While a single kink seems to be sufficient to stabilize a torsionally relaxed minicircle, two kinks seem to be preferable when an increased linking number leads to an initial torsional stress. Some of the kinks involve two consecutive base-pair steps with destruction of the intervening base pair, but no evidence of more extensive base unpairing is seen during the simulations. While other conformational events may occur on time scales much slower than the submicrosecond duration of these simulations, our findings suggest that kinking remains a feasible route for relaxing elastic energy in strongly bent DNA. We also note that kinks act like a door hinge with a strong preference for their direction of opening, namely toward the minor groove. Whether the magnitude of opening is stiff or comparatively soft is less clear. The presence of even a single kink has a significant impact on the overall conformation of the minicircle, particularly on its rotational register

(i.e., which face of the DNA is turned inwards toward the bend at a particular base pair).

Results and Discussion

Minicircles with linking numbers *Lk* = 9 and *Lk* = 8 (or L9 and L8) were chosen to obtain both torsionally relaxed and torsionally stressed initial configurations. While DNA in solution is known to have a sequence-averaged twist of roughly 34.5° (implying that a close-to-circular 94 bp minicircle will have exactly nine helical turns and so be torsionally relaxed) it is also known that the Cornell et al. (parm94) force field (Cornell et al., 1995) underestimates DNA twist and yields a sequence-averaged value of around 30°. This implies that when the DNA axis lies close to a (geometrical) circle the *Lk* = 9 minicircle will be positively supercoiled by roughly one turn, while an *Lk* = 8 minicircle is torsionally relaxed. This was indeed found to be the case in the present simulations. Although a later version of the AMBER force field partially corrects the tendency to undertwist, it is known to have other drawbacks, which led us to choose parm94, in line with recent extensive molecular dynamics studies of sequence effects in DNA (Beveridge et al., 2004; Dixit et al., 2005). Despite this discrepancy of twist with experiment, simulating both relaxed and torsionally overwound minicircles gives us the possibility of studying the role of kinks in relaxing different degrees of imposed torsional stress.

For each of the two linking numbers, two different starting structures, with either "rough" (r) or "smooth" (s) initial conformations were used (see Experimental Procedures). The corresponding trajectories will be referred to as L9r, L9s, L8r, and L8s, respectively. All trajectories were extended to at least 80 ns. In addition, because of the absence of any short-term kink formation, the simulation L8s was branched after 43 ns of simulation, giving rise to two distinct trajectories, L8sa and L8sb.

We begin by describing the evolution of the global conformation of the simulated minicircles. Figure 1 shows the conformations of L9s and L8sa after 80 ns of simulation. These configurations are representative of seemingly stable shapes obtained after kink formation in each of the two linking number families. (The shapes can be better appreciated from the three-dimensional representations provided in movies and PDB files; see Supplemental Data available with this article online.) The L8sa simulation stays close to planar but with a single kink (marked by the arrow in Figure 1), which is associated with a large deformation to a teardrop shape, with the kink located at the tip. The L8r simulation is similar, whereas L8sb (without kinks) remains virtually circular.

In contrast, the L9s shape exhibits substantial writhe, as might be expected given that the initial circular configuration is torsionally stressed. More specifically, the highly deformed L9s configuration involves a shorter, close-to-straight segment, of approximately 38 bp, capped at either end with kinks (marked by arrows) that are joined with a longer, highly writhed, S-shaped segment that in this projection, attaches at the top and bottom of the straight segment. We refer to this characteristic shape as a swiss roll. The L9r simulation also assumes a swiss-roll shape, although there are a total of three kinks

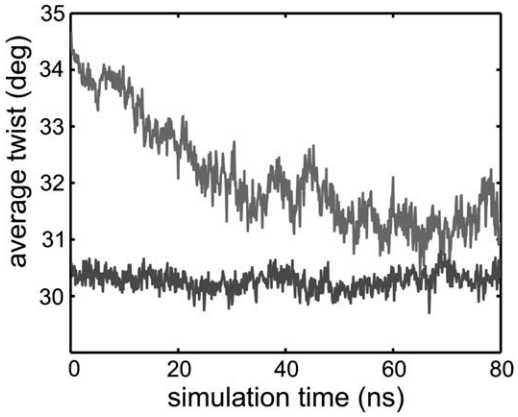

Figure 2. Time Evolution of Sequence-Averaged Twist

L9s (upper curve) and L8sa (lower curve). The average twist in L9s shows a gradual overall decrease until it stabilizes after about 50 ns, corresponding to an initial increase in writhe of the configuration. In contrast, the average twist in L8sa remains stable over the entire simulation corresponding to nearly constant, vanishing writhe.

with two of them (following base pairs 1 and 4) very close to each other forming a single, compound kink, and the length of the shorter, nearly straight segment is approximately 42 bp. Figure 2 confirms that while average twist fluctuates around a constant value in the quasiplanar L8sa simulation, it decreases monotonically during the first half of the L9s simulation, corresponding to the build up of positive writhe.

Figure 3 presents time series of two local conformational parameters, namely roll and propeller angles, in the L9s and L8sa simulations. The figure reveals that initially, all roll and propeller values along the minicircle lie within standard ranges. However, as time progresses, certain base-pair steps adopt large negative rolls, in some cases accompanied by base pairs with large positive propellers. A more detailed examination revealed the formation of kinked structures at these locations (see Figure 4). Note that the L9s simulation shows a nascent kink after 5 ns at bp 10, with temporary disruption of pairs 10 (GC) and 11 (AT), but this disappears after 25 ns. All other kinks, once formed, remain stable until the end of the simulations. Figure 5 provides plots of the time-average values of the six helical parameters at each of the 94 bp steps. Kinks again stand out. Figures analogous to Figures 1–3 and 5 for the remaining simulations L9r, L8sb, and L8r are provided in the Supplemental Data.

The kinks seen in our simulations can be divided into two types. Type I (which predominates) involves a negative roll angle between two consecutive, intact base pairs. Negative roll implies opening the base-pair step on the major groove side, resulting in kinking toward the minor groove. The kink measurement described in the Experimental Procedures section leads to kink angles of 90°–110° for type I kinks. Type I kinks are observed following bp 35 in L9s (see Figure 4) and bp 94 in L8sa. (We stress that in our simulation protocol for these cyclized molecules, step 94 between bp 94 and bp 1 is treated identically to all other steps.) A type II kink, which is observed only in the L9s simulation at bp 73–75 (see Figure 4), involves three consecutive

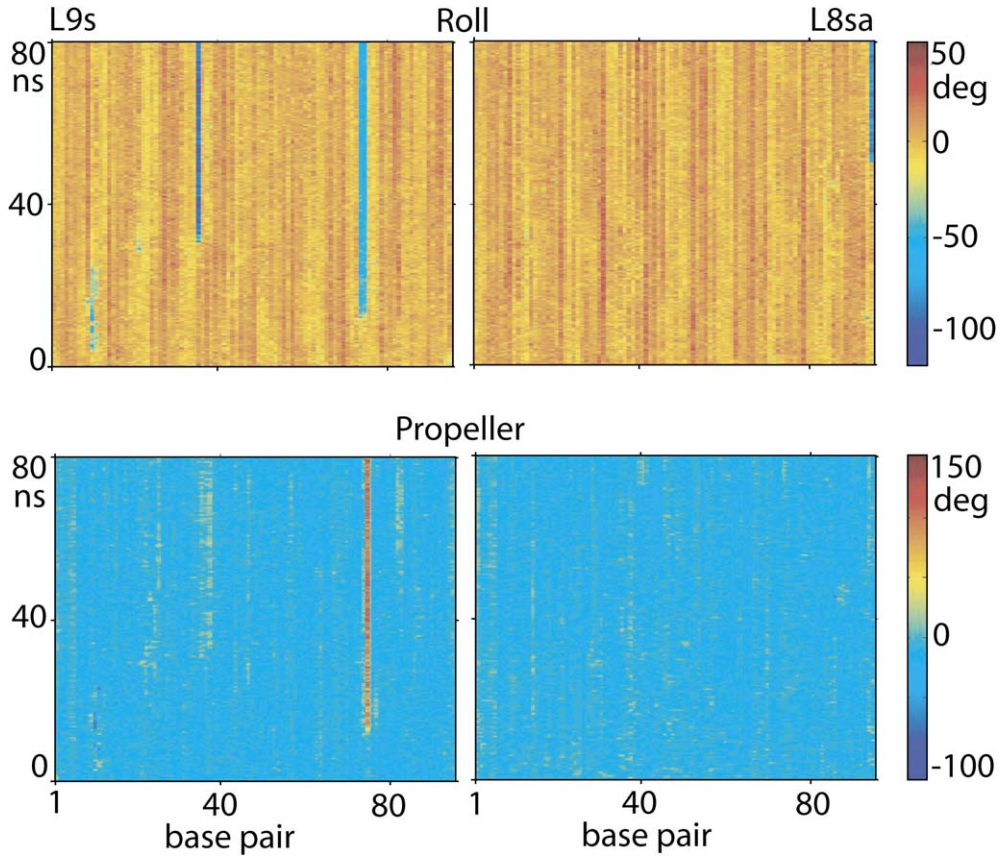

Figure 3. Time Evolution of Roll and Propeller

L9s (left) and L8sa (right). In each case, the base-pair steps (for roll) or base pairs (for propeller) are numbered from left to right along the horizontal axis, and the simulation time increases upwards along the vertical axis. Color bars at the right indicate the range of values in degrees. The highly contrasted, vertical stripes signal kink formation, specifically at bp 10, 35, and 73 in L9s and at bp 94 in L8sa. We note that our bp numbering convention follows that of Cloutier and Widom (2004), and the L8sa simulation exhibits kink formation at the highest indexed step, which occurs between bp 94 and bp 1. Consequently, it should be emphasized that in our simulation protocol for these cyclized molecules, nothing distinguishes step 94 from any other step, other than the surrounding bp sequence.

base pairs. The hydrogen bonding of the two flanking pairs is conserved, while the central pair is broken, and its bases are stacked on the 5′ neighboring bases of the corresponding strand. The two intact pairs 73 and 75 are again kinked toward the minor groove with a kink angle of roughly 120°.

The occurrence and geometry of all observed kinks are summarized in Table 1. These results suggest that while there is apparently no simple rule concerning the sequence dependence of kinks, pyrimidine-purine (YpR) steps are preferred for kinking, and CG steps are the most frequent. Surprisingly, no kink is seen at weakly stacked TpA steps, although such steps are common in the simulated sequence.

The type I kink, which dominates our simulations, closely resembles that described by Crick and Klug (Crick and Klug, 1975). They proposed a structure with two consecutive, intact base pairs kinked into the minor groove by an angle that "is easily made more than 90°, but approaches 100° with difficulty." They note, in particular, that kinks into the major groove would have "a smaller angle of kink and seem rather awkward to build." These predictions are all perfectly consistent with our simulations.

Crick and Klug also predicted that the backbone torsion angle γ (05′-C5′-C4′-C3′) at the kink should be in the *t* instead of the standard *g+* conformation (i.e., approximately 180° instead of 50°). This type of backbone flip has recently been detected in simulations of naked DNA with the parm94 force field (Beveridge et al., 2004; Dixit et al., 2005). In line with these findings, γ transitions in our simulations build up with time, with, at the end of the simulations, roughly 70% of all steps flipped in at least one strand. Observation of the behavior of γ at the kinks reveals that every type I kinked step is associated with at least one of the two γ torsions adopting the *t* conformation. The type II kink in L9s also has at least one strand in *t*, namely at step 73. There is however no simple relationship between the occurrence of kinks and the values of the backbone torsion angles α (O3′-P-O5′-C5′) or β (P-O5′-C5′-C4′), which are often linked to transitions in γ. These observations suggest that γ-flipped conformations are necessary for kinking, notably since these flips accompany the formation of kinks (with only one exception) at a time when only 20%–45% of γ transitions have occurred overall.

It is important to stress that the kinks discussed above are by far the largest conformational perturbation away

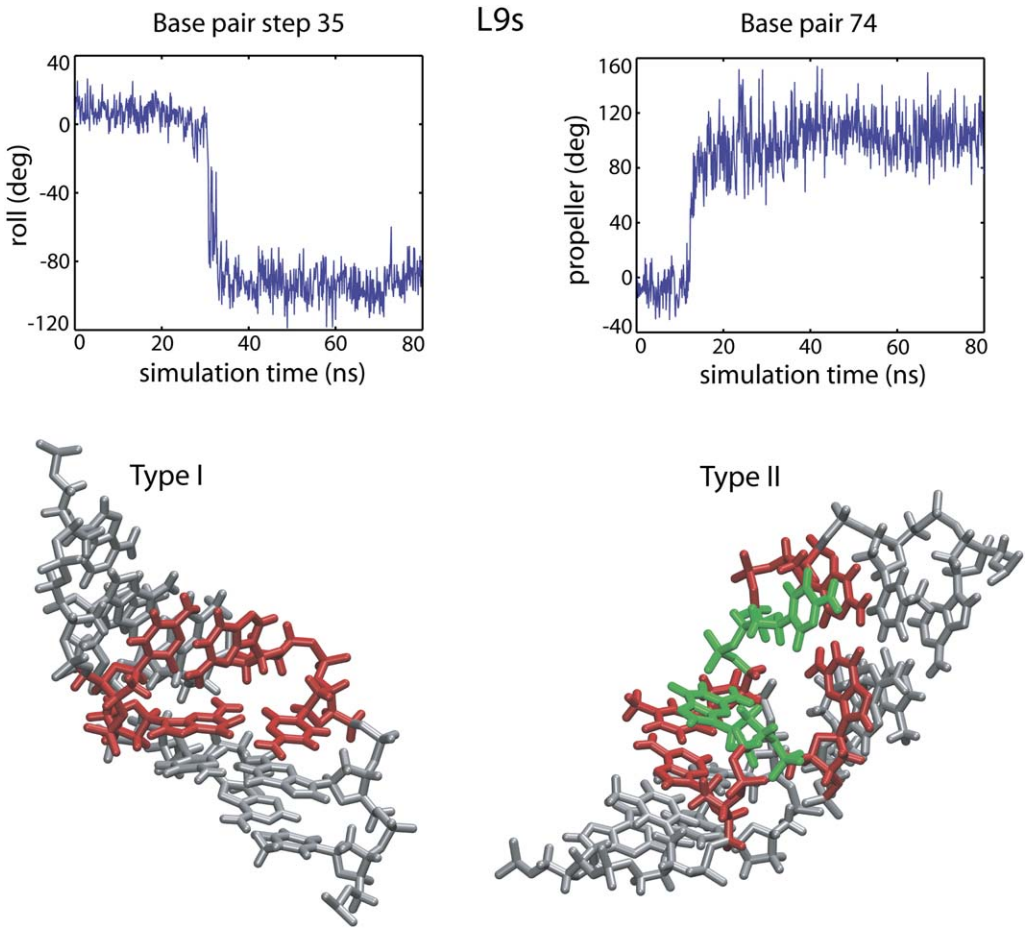

Figure 4. Kink Conformations

The upper time series show the sudden changes that occur in roll and propeller when kinks form. The lower diagrams show close-up three-dimensional views of type I and type II kinks (taken from L9s at 80 ns and at step 35 and at steps 73–74, respectively, in each case looking into the major groove). Kinked base pairs shown in red with, for the type II kink, the broken central pair in green.

from a double helical structure that occur during these minicircle simulations. In particular, we see no evidence of the locally unpaired regions or bubbles that have been suggested as an alternative way of relaxing bending stress (Yan et al., 2005; Yan and Marko, 2004). Apart from the unpairing observed with the central pair of the type II kink, we only rarely observe isolated base pairs that become damaged. Several base pairs are transiently unpaired during the simulation, but the pairing is recovered spontaneously within 3–5 ns. Two AT pairs, however, stayed unpaired until the end of the simulations. One is pair 38 in L9r, which, at the end of the simulation, is unpaired, but planar, with thymine rotated into the major groove. A careful inspection of the trajectory revealed that before adopting this structure, the pair and its neighbors went through a series of transient conformations (over the last 8 ns of simulation), which resemble an attempt to kink into the major groove. The other unpairing occurs at step 85 in L8r where the two bases are stacked on one another within the helix. Prior to adopting this conformation, the pair and its neighbors formed distorted structures during the last 20 ns of the trajectory, which on several occasions, resembled type II kinks.

Finally, we turn to the rotational register of the minicircles (Sanghani et al., 1996). As discussed above, in both L9 and L8 simulations both type I and type II kinks show strong orientational preferences for bending toward the minor groove. The idea of register relates the minor groove direction at a given bp to the overall shape of deformation. In the nearly planar L8 minicircles, a Fourier analysis of the roll angles (Bishop, 2005) (see Experimental Procedures for further details) allows the rotational register of the minicircle to be sharply identified, and it can be observed that indeed all kinks are well aligned with the direction of maximum bend, that is toward the center of the minicircle. As shown in Figure 6, for L8sa, the register measured at step 94 initially fluctuates between 100° and 200°. However, after the kink forms, the register stabilizes around a mean value of 126° with a standard deviation of 12°. In contrast, at the same location and over the whole simulation the unkinked L8sb shows broad fluctuations in register ranging from 50° to 200°. L8r adopts a kinked state early in the simulation (see Table 1) and consequently, like the kinked stage of L8sa, shows limited register fluctuations for the first 60 ns of simulation with an average value at the kink position (step 24) of 162° and a standard

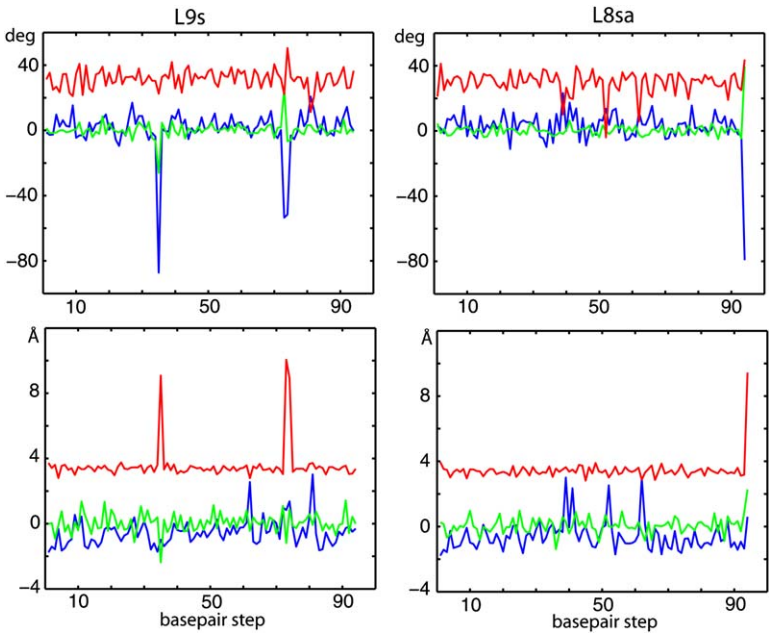

Figure 5. Time Averages of Helical Parameters as a Function of bp Step

L9s (left) and L8sa (right). Top: tilt (green), roll (blue), and twist (red); bottom: shift (green), slide (blue), and rise (red). Averages were taken over the last 5 ns of simulation. Note that due to periodicity along the closed minicircles, step 94 (far right) is followed by step 1 (the left extremity). The three kinks stand out as having large negative roll values, with associated large rises and exceptional values of tilt. The secondary features close to bps 60 and 80 in L9s and bps 40, 50, and 60 in L8sa with steps of unusually high slides and associated low twists remain to be investigated more fully.

deviation of 13°. As mentioned above, the last 20 ns of the L8r simulation is marked by another conformational change with bp 85 breaking. A similar analysis of register for the *Lk* = 9 minicircles was indecisive since their highly nonplanar centerlines lead to more complex Fourier spectra of the roll angles.

Conclusions

A series of five atomic resolution, explicit solvent, molecular dynamics simulations of a 94 bp DNA minicircle have been performed with four different starting conformations. The trajectories each lasted from 80–85 ns. The two torsionally stressed, *Lk* = 9, simulations both evolved to the double kink, highly writhed structure that we term a swiss roll, independent of whether the initial data was more or less smoothed. The three torsionally unstressed, link *Lk* = 8 simulations twice evolved into a single kink, teardrop shape and once remained unkinked. The predominant kink type consists of two consecutive, intact base pairs kinked toward the minor groove by 90°–110°, a structure closely resembling that predicted by Crick and Klug. In one case, we observe another type of kink involving three consecutive base pairs, where the central pair is broken with its bases stacked on the 5′ neighboring bases. This structure again results in kinking toward the minor groove. These kinks appear to be stiff in direction. It is harder to assess stiffness of the opening angle of the kink; while the standard deviations of kink angle given in Table 1 are quite small, it is possible that the small variations are due to coupling to the overall shape of the minicircle rather than due to a local stiffness of the opening angle itself. The number of kinks formed is related to the torsional stress of the minicircle, with torsionally relaxed states favoring a single kink and positively supercoiled states favoring two kinks. Unsurprisingly, the kinks are localized at positions of high curvature in the overall shape of the minicircle. Formation of a kink suppresses subsequent fluctuations in the rotational register. No evidence of unpaired regions is found, although individual base pairs can be transiently or (in two cases) permanently broken. Our results suggest that DNA kinking may occur in the absence of bound proteins. They also suggest that elastic models of DNA in high curvature regimes should

Table 1. Kinks Observed during the Simulations

Simulation	Type	Appearance (ns)	Base-Pair Step	Angle (°)	Direction (°)
L9s	I	31	35 (CG)	103 (8)	208 (14)
	II	12	73–74 (AGG)	116 (7)	249 (10)
L9r	I	14	1 (GG)		
	I	9	4 (CG)	108 (8)	290 (9)
	I	24	45 (CG)	105 (7)	225 (14)
L8sa	I	50	94 (CG)	91 (9)	214 (12)
L8sb	—	—			
L8r	I	6	24 (CA)	99 (9)	231 (8)

Appearance refers to the simulation time (ns) at which the kink formed. Averages (with standard deviations in parentheses) for kink angle and direction (in degrees) were calculated over the interval between 60 and 80 ns of each simulation. The 5′ and 3′ segments used for the measurements (see Experimental Procedures) were chosen such that for type I, they include, respectively, the 5′ and 3′ pair of the kinked step, and for type II, they include the intact pairs at the kink location (73 and 75, respectively). The two adjacent kinks in L9r (at steps 1 and 4) were treated as one so that the 5′ segment ends with base pair 1 and the 3′ segment starts with base pair 5.

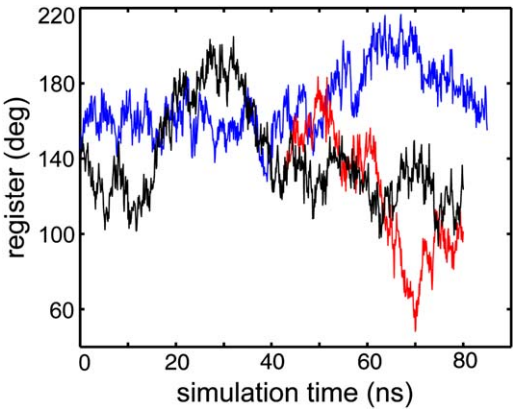

Figure 6. Time Evolution of Register of Fixed bp Steps for Link 8 Minicircles

L8r, blue; L8sa, black; L8sb, red. Register is calculated for step 24 in L8r, and step 94 in L8sa, which represent the kink positions in each minicircle. Step 94 was also taken in L8sb. The L8sa simulation develops a kink at 50 ns; afterwards, the register exhibits much less variation than that in L8sb where no kink has formed. In the case of L8r, the kink forms early in the simulation (at 5 ns), and the register remains relatively stable until the formation of another structural deformation at around 60 ns (see text).

take into account the possibility of localized kinks that are stiff in direction.

Experimental Procedures

We studied the 94 bp DNA minicircle with the sequence showing the highest J factor (closure probability) reported in the study of Cloutier and Widom (Cloutier and Widom, 2004). Explicitly, the sequence is dGGCCGGGTCG TAGCAAGCTC TAGCACCGCT TAAACGCACG TACGCGCTGT CTACCGCGTT TTAACCGCCA ATAGGATTAC TTACTAGTCT CTAC (a space has been inserted every 10 bp for readability). Initial structures with close-to-circular centerlines were created with JUMNA (Lavery et al., 1995), a nucleic acid modeling program that, due to the combined use of helical and internal coordinates, can build DNA fragments with regular superhelical structures. In the present case, a closed, planar minicircle was created, starting with standard rise and twist values of 3.38 Å and 34.5°, respectively, corresponding to linking number 9, as would be expected for 94 bp with a helical repeat of 10.5 bp. This structure was subjected to conjugate gradient energy minimization before being transferred to AMBER 7.0 (Case et al., 2002) for molecular dynamics simulations. For reasons explained above, we also built a second form of this minicircle with twist values reduced to 30.6°, corresponding to linking number 8. For each of the two linking numbers, two different starting structures were used for the dynamic simulations. In the first, the energy of the system was subjected to only limited minimization, thus preserving the irregular helical and backbone parameters created during the backbone closure of the initial JUMNA construction phase. These structures are referred to as "rough." In order to verify that kink formation and location was not being unduly influenced by the irregularity of the starting conformations, a second initial structure of each link was obtained with much more extensive minimization, leading to more regular initial backbone and helical parameters. These simulations are referred to as "smooth."

The dynamic simulations were performed with the AMBER 7.0 suite of programs (Case et al., 2002) and the Cornell et al. parm94 force field (Cornell et al., 1995). Potassium ions (188 in total) were added to neutralize the negative charge of the DNA minicircle, and the system was solvated in an octahedral periodic box with explicit water molecules by using the TIP3P water model (Jorgensen, 1981). The positions of the ions were then randomly exchanged with water molecules to avoid effects related to the initial ion placement. The system was equilibrated by a series of energy minimizations and short molecular dynamics runs, gradually relaxing positional restraints on the DNA atoms with the *SANDER* module of AMBER 7.0. The production run, performed with the *PMEMD* module, consisted of 80 ns of unrestrained molecular dynamics simulation, except the L8r trajectory, which was prolonged to 85 ns. The system was kept at a constant temperature of 300 K and at a constant pressure of 1 atm with the Berendsen thermostat and barostat (Berendsen et al., 1984). The coupling constants to the temperature and pressure reservoirs were 5 ps. More details of the protocol are described elsewhere (Beveridge et al., 2004).

Snapshots containing the atomic coordinates from the simulated trajectories were saved at 1 ps intervals. The DNA conformation in each snapshot was extracted and analyzed with CURVES (Lavery and Sklenar, 1988; Lavery and Sklenar, 1989) to obtain time series of conformational parameters, e.g., the roll and propeller angles shown in Figure 3.

An ad hoc tool was developed to investigate the geometry of the observed kinks. Both the kink angle and the direction of the kinks were measured. First, a linear helical axis was calculated with CURVES for the 10 bp segments preceding and following the kink (i.e., on its 5′ and 3′ sides with respect to the strand whose sequence is given above). The kink angle (in the range 0°–180°) is then defined as the angle between these two axes. The kink direction (in the range 0°–360°) was measured as the angle between the helical axis of the 3′ segment and the pseudodyad axis of the last base pair of the 5′ segment, after both had been projected into a plane perpendicular to the helical axis of the 5′ segment. The kink direction was measured as right-handed rotation, with 0° corresponding to the major groove direction for the base pair preceding the kink site. In order to correct the pseudodyad reference to the middle of the kink, one should subtract roughly 15° (i.e., half of the base pair twist) from the measured kink direction for type I, and 30° for type II kinks.

We also monitored the rotational register of the minicircles, a quantity specifying which face of the DNA points toward the inside of the minicircle (Sanghani et al., 1996). This was carried out by a Fourier analysis of the roll angles following Bishop (2005). For the *Lk* = 8, relatively planar, minicircle configurations, the discrete Fourier spectrum exhibits a dominant peak with the expected 8-fold periodicity corresponding to a Fourier mode of the form $A_8\cos\phi_k$, $A_8(t)>0$, where $\phi_k=(360\times8/94)(k-1)+\phi_0(t)$, with $k=1,2,\ldots,94$ being the bp step index. For each t, $\phi_k(t)$ reflects the variation of the roll angles along the minicircle with the maximum positive rolls occurring for the values of k at which $\phi_k(t)\cong0$, while $\phi_k(t)\cong180$ implies maximum negative roll. The assumption is that these maxima and minima occur for bp indices at which respectively the major and minor grooves face inwards toward the center of the nearly circular configuration. The variation in time of the register angle at a fixed bp index k can then be defined via the phase angle $\phi_0(t)$, as shown in Figure 6. A similar analysis was not possible for the *Lk* = 9 minicircles since their highly nonplanar centerlines lead to more complex Fourier spectra of the roll angles with no fixed dominant mode independent of t.

Supplemental Data

Supplemental Data include figures that provide for simulations L9r, L8r, and L8sb the analogs of Figures 1–3 and 5 of the main text. It also includes the final structures of the five simulations, in PDB format and as movies. Supplemental Data are available at http://www.structure.org/cgi/content/full/14/10/1527/DC1/.

Acknowledgments

F.L. and J.H.M. acknowledge support provided by the Swiss National Science Foundation and from a research collaboration between the Ecole Polytechnique Federale de Lausanne and Hewlett-Packard. R.L. acknowledges the support of the Centre National de la Recherche Scientifique. Part of the simulations were done on the Cray XD1 computer in the Zuse Institute Berlin (ZIB); we thank ZIB and Dr. Thomas Steinke for generous help. The authors also thank Jon Widom for useful preliminary discussions and providing the sequence that was simulated, Leesa Heffler for help with preparing the movies presented in the Supplemental Data, and the referees for their most useful and constructive comments.

Received: May 23, 2006
Revised: August 2, 2006
Accepted: August 4, 2006
Published: October 10, 2006

References

Allemand, J.F., Bensimon, D., Lavery, R., and Croquette, V. (1998). Stretched and overwound DNA forms a Pauling-like structure with exposed bases. Proc. Natl. Acad. Sci. USA *95*, 14152–14157.

Becker, N.A., Kahn, J.D., and Maher, L.J., III. (2005). Bacterial repression loops require enhanced DNA flexibility. J. Mol. Biol. *349*, 716–730.

Berendsen, H.J.C., Postma, J.P.M., van Gunsteren, W.F., DiNola, A., and Haak, J.R. (1984). Molecular dynamics with coupling to an external bath. J. Chem. Phys. *81*, 3684–3690.

Beveridge, D.L., Barreiro, G., Byun, K.S., Case, D.A., Cheatham, T.E., III, Dixit, S.B., Giudice, E., Lankas, F., Lavery, R., Maddocks, J.H., et al. (2004). Molecular dynamics simulations of the 136 unique tetranucleotide sequences of DNA oligonucleotides. I. Research design and results on d(CpG) steps. Biophys. J. *87*, 3799–3813.

Bishop, T.C. (2005). Molecular dynamics simulations of a nucleosome and free DNA. J. Biomol. Struct. Dyn. *22*, 673–686.

Bustamante, C., Marko, J.F., Siggia, E.D., and Smith, S. (1994). Entropic elasticity of lambda-phage DNA. Science *265*, 1599–1600.

Case, D.A., Pearlman, D.A., Caldwell, J.W., Cheatham, T.E., III, Wang, J., Ross, W.S., Simmerling, C.L., Darden, T.A., Mer, K.M., Stanton, R.V., et al. (2002). AMBER 7 (San Francisco, CA: University of California, San Francisco).

Cloutier, T.E., and Widom, J. (2004). Spontaneous sharp bending of double-stranded DNA. Mol. Cell *14*, 355–362.

Cloutier, T.E., and Widom, J. (2005). DNA twisting flexibility and the formation of sharply looped protein-DNA complexes. Proc. Natl. Acad. Sci. USA *102*, 3645–3650.

Cluzel, P., Lebrun, A., Heller, C., Lavery, R., Viovy, J.L., Chatenay, D., and Caron, F. (1996). DNA: an extensible molecule. Science *271*, 792–794.

Cornell, W.D., Cieplak, P., Bayly, C.I., Gould, I.R., Merz, K.M.J., Ferguson, D.M., Spellmeyer, D.C., Fox, T., Caldwell, J.W., and Kollman, P.A. (1995). A second generation force field for the simulation of proteins, nucleic acids and organic molecules. J. Am. Chem. Soc. *117*, 5179–5197.

Crick, F.H., and Klug, A. (1975). Kinky helix. Nature *255*, 530–533.

Dixit, S.B., Beveridge, D.L., Case, D.A., Cheatham, T.E., III, Giudice, E., Lankas, F., Lavery, R., Maddocks, J.H., Osman, R., Sklenar, H., et al. (2005). Molecular dynamics simulations of the 136 unique tetranucleotide sequences of DNA oligonucleotides. II: sequence context effects on the dynamical structures of the 10 unique dinucleotide steps. Biophys. J. *89*, 3721–3740.

Doi, M., and Edwards, S.F. (1985). Theory of Polymer Dynamics (Oxford: Oxford University Press).

Drew, H.R., Weeks, J.R., and Travers, A.A. (1985). Negative supercoiling induces spontaneous unwinding of a bacterial promoter. EMBO J. *4*, 1025–1032.

Du, Q., Smith, C., Shiffeldrim, N., Vologodskaia, M., and Vologodskii, A. (2005). Cyclization of short DNA fragments and bending fluctuations of the double helix. Proc. Natl. Acad. Sci. USA *102*, 5397–5402.

Jorgensen, W.L. (1981). Transferrable intermolecular potential functions for water, alcohols and ethers. Application to liquid water. J. Am. Chem. Soc. *103*, 335–340.

Kratky, O., and Porod, G. (1949). Rontgenuntersuchung geloster fadenmolekule. Recl. Trav. Chim. Pays Bas *68*, 1106–1122.

Lavery, R., and Sklenar, H. (1988). The definition of generalized helicoidal parameters and of axis curvature for irregular nucleic acids. J. Biomol. Struct. Dyn. *6*, 63–91.

Lavery, R., and Sklenar, H. (1989). Defining the structure of irregular nucleic acids: conventions and principles. J. Biomol. Struct. Dyn. *6*, 655–667.

Lavery, R., Zakrzewska, K., and Sklenar, H. (1995). JUMNA (junction minimization of nucleic acids). Comput. Phys. Commun. *91*, 135–158.

Manning, R.S., Maddocks, J.H., and Kahn, J.D. (1996). A continuum rod model of sequence-dependent DNA structure. J. Chem. Phys. *105*, 5626–5646.

Protozanova, E., Yakovchuk, P., and Frank-Kamenetskii, M.D. (2004). Stacked-unstacked equilibrium at the nick site of DNA. J. Mol. Biol. *342*, 775–785.

Richmond, T.J., and Davey, C.A. (2003). The structure of DNA in the nucleosome core. Nature *423*, 145–150.

Sanghani, S.R., Zakrzewska, K., Harvey, S.C., and Lavery, R. (1996). Molecular modelling of (A4T4NN)n and (T4A4NN)n: sequence elements responsible for curvature. Nucleic Acids Res. *24*, 1632–1637.

Shimada, J., and Yamakawa, H. (1984). Ring-closure probabilites for twisted wormlike chains. Application to DNA. Macromolecules *17*, 689–698.

Smith, S.B., Cui, Y., and Bustamante, C. (1996). Overstretching B-DNA: the elastic response of individual double-stranded and single-stranded DNA molecules. Science *271*, 795–799.

Strick, T.R., Allemand, J.F., Bensimon, D., Bensimon, A., and Croquette, V. (1996). The elasticity of a single supercoiled DNA molecule. Science *271*, 1835–1837.

Travers, A. (2005). DNA dynamics: bubble 'n' flip for DNA cyclisation? Curr. Biol. *15*, R377–R379.

Vilar, J.M., and Saiz, L. (2005). DNA looping in gene regulation: from the assembly of macromolecular complexes to the control of transcriptional noise. Curr. Opin. Genet. Dev. *15*, 136–144.

Vologodskii, A. (1994). DNA extension under the action of an external force. Macromolecules *27*, 5623–5625.

Wiggins, P.A., Phillips, R., and Nelson, P.C. (2005). Exact theory of kinkable elastic polymers. Phys. Rev. E Stat. Nonlin. Soft Matter Phys. *71*, 021909.

Yan, J., and Marko, J.F. (2004). Localized single-stranded bubble mechanism for cyclization of short double helix DNA. Phys. Rev. Lett. *93*, 108108.

Yan, J., Kawamura, R., and Marko, J.F. (2005). Statistics of loop formation along double helix DNAs. Phys. Rev. E Stat. Nonlin. Soft Matter Phys. *71*, 061905, Erratum: Phys. Rev. E Stat. Nonlin. Soft Matter Phys. *72*(5 Part 2), 2005.

Zhang, Y., and Crothers, D.M. (2003). Statistical mechanics of sequence-dependent circular DNA and its application for DNA cyclization. Biophys. J. *84*, 136–153.